Available online at www.sciencedirect.com
ScienceDirect
Proceedings of the Combustion Institute 35 (2015) 3529–3536
Proceedings of the Combustion Institute
www.elsevier.com/locate/proci

Subgrid scale modelling for MILD combustion

Y. Minamoto *, N. Swaminathan

Department of Engineering, University of Cambridge, Trumpington Street, Cambridge CB2 1PZ, UK

Available online 27 July 2014

Abstract

A simple closure for filtered reaction of a reaction progress variable is analysed in this study using explicitly filtered DNS data of turbulent MILD combustion of methane for Large Eddy Simulation (LES). The conditional averages of major and minor species mass fractions, and reaction rate constructed from the DNS data along with those obtained using flamelet and Perfectly Stirred Reactor (PSR) models suggest that the PSR can serve as a good canonical reactor for MILD combustion modelling. The flamelet predictions of reaction rate are observed to be poor because it does not include effects of flame interactions, which are abundant in the MILD combustion. The PSR solution obtained over a wide range of residence time along with presumed beta sub-grid PDF seems a reasonable closure for the filtered reaction rate for the LES filter size greater than three flame thermal thicknesses. Both spatial variations and joint PDF of modelled and DNS values of filtered reaction rates are analysed.

Keywords: Direct Numerical Simulation (DNS); Exhaust Gas Recirculation (EGR); Moderate or Intense Low-oxygen Dilution (MILD); Flameless Combustion; SGS modelling

1. Introduction

Due to the need for combustion systems with improved efficiency and reduced emissions, alternative combustion technologies are being constantly explored to meet these requirements. Although fuel-lean premixed combustion can meet these requirements it is highly susceptible to thermo-acoustic instability. Moderate or Intense Low-oxygen Dilution (MILD) combustion is another technology employing diluted and preheated reactants which can overcome the shortcoming of lean premixed combustion. The reactant temperature, T_r, is higher than reactant mixture's autoignition temperature T_{ign} and the temperature rise, $\Delta T = T_p - T_r$, is smaller than T_{ign} for combustion under typical MILD conditions. The MILD combustion conditions can be achieved using Exhaust or Flue Gas Recirculation (EGR or FRG) or staged fuel injection methods.

Direct photographs of MILD combustion from previous experimental studies [1–3] suggest spatially uniform and steady combustion. A possible theoretical explanation for this uniform combustion has been offered on the basis of two-stage evolution, where fuel-rich combustion in diluted oxidiser is followed by homogeneous combustion of partially oxidised fuel [1]. More theoretical analyses of methane oxidation under diluted conditions have been conducted by using a Perfectly Stirred Reactor (PSR) model [4,1,5–8] suggesting that combustion

* Corresponding author.
E-mail address: yminamo@sandia.gov (Y. Minamoto).

http://dx.doi.org/10.1016/j.proci.2014.07.025

in diluted conditions may be seen as turbulent combustion in distributed regime. Although laser thermometry images in [9,2,10] suggested distributed regime combustion, OH Planar Laser Induced Fluorescence (PLIF) images in the same studies show the presence of thin reaction zones. It has been recently pointed out [11] that frequent interactions of thin reaction zones in MILD combustion produce conditions similar to distributed regime combustion.

Modelling of MILD combustion is important from the application's point of view. The Eddy Dissipation Concept (EDC) is extensively used in previous modelling studies of MILD combustion using both Reynolds Averaged Navier–Stokes (RANS) [12–17] and Large Eddy Simulation (LES) [18] approaches. The computational results from these studies compare reasonably to experimental results, suggesting that the EDC model is satisfactory. However, its fundamental assumption of a homogeneous reactor within fine structures of turbulent kinetic energy dissipation has not been verified for MILD combustion. It is important to note at this juncture that the distributed regime of combustion does not result from only turbulence–flame interaction, but also by interactions of reaction zones [11] in MILD combustion. Large Eddy Simulations involving a presumed sub-grid probability density function (PDF) with canonical reactors have also been explored [19,20]. The filtered reaction rate, $\overline{\omega}$, in this approach is written as

$$\overline{\omega} = \int_0^1 \omega_L(c) P_\Delta(c)\, dc, \tag{1}$$

using a sub-grid PDF, $P_\Delta(c)$, for a reaction progress variable (RPV) c by presuming the PDF shape for given values of Favre filtered RPV $\widetilde{c}$ and its sub-grid variance σ_c^2. The reaction rate $\omega_L(c)$ may be assumed to depend only on c and is taken from an appropriate canonical model, either a PSR [19] or a steady flamelet [20]. Thus, precomputed and tabulated values for $\overline{\omega}$ can be used during LES using look-up table approach. However, choice for this model reactor is unclear in the light of experiments cited above, which show both distributed and flamelets combustion. Thus, a careful investigation is warranted to improve our understanding of turbulent MILD combustion and to guide filtered reaction rate modelling.

This study attempts to provide a guidance for SGS modelling of reaction rate in MILD combustion using Direct Numerical Simulation (DNS). The aim is to develop and validate a representative canonical reactor to model $\overline{\omega}$ using Eq. (1) for turbulent MILD combustion. The organisation of this paper is as follows. The DNS method and MILD combustion condition investigated in this study are briefly described in Section 2. The details of analysis are presented in Section 3 and results of this analysis are discussed in Section 4. *A priori* assessment of filtered reaction rate model is discussed in Section 5 by directly comparing modelled $\overline{\omega}$ with those extracted from the DNS results. The conclusions are summarised in Section 6.

2. DNS of MILD combustion

Turbulent MILD combustion of methane–air mixture at atmospheric pressure inside a cubic domain has been simulated [11,21] directly using a DNS code, SENGA2 [22]. This code solves fully compressible conservation equations for mass, momentum, internal energy and species mass fractions, Y_i, for turbulent reacting flows. The governing equations are discretised on a uniform mesh employing a tenth order central difference scheme which gradually reduces to a fourth order scheme near boundaries. The integration in time is achieved using a third order Runge–Kutta scheme. The methane–air combustion kinetics is modelled using a skeletal mechanism including 16 species and 25 elementary reactions [23]. The transport and thermo-chemical properties of the mixture and individual species are temperature dependent and these species have non-unity Lewis numbers as they have different mass diffusivities.

The fuel and air are usually fed through a high momentum jet into a stream of exhaust gases to achieve conditions for MILD combustion. The high temperature for either fuel or air is usually achieved by recovering heat in the exhaust stream. The time available for air, fuel and exhaust gases to mix is usually short in a typical MILD combustion arrangement. This results in inhomogeneous mixtures made of unburnt and burnt gases. These physical processes are included in the DNS through a two-stage strategy detailed in Refs. [11,21,24]. In the first stage, mixing between fresh and exhaust gases is simulated directly inside a periodic domain without chemical reactions, and the duration of this DNS is about one large eddy turnover time which is much shorter than the autoignition delay time for the given mixture conditions, but long enough to have partially premixed fresh and exhaust gases [24]. The turbulence Reynolds number, $\mathrm{Re}_t = u' l_0/\nu = 96.1$, where u', l_0 and ν are respectively the turbulence intensity, integral length scale and kinematic viscosity of reactant mixture, is similar to those in previous experimental studies [25–27]. In the second stage, this inhomogeneous mixture is used as the initial and inflowing mixture for the combustion simulation. This inflowing mixture has $u' = 16.4\,\mathrm{m/s}$ and $l_0 = 1.48\,\mathrm{mm}$.

The volume averaged temperature, T_m, of the inflowing mixture field is 1500 K while $T_r = T_m \pm 0.02\,T_m$ resulting from mixing of reactants

and exhaust gases. The maximum, $X^{\max}_{O_2,r}$, and averaged, $\langle X_{O_2,r}\rangle$, mole fractions of oxygen in reactant mixture are respectively 0.035 and 0.025 which are similar to those for a typical MILD combustion condition [5]. The stoichiometric, ξ_{st}, and averaged, $\langle\xi\rangle$, values of Bilger mixture fraction are 0.010 and 0.008 respectively because of intense dilution. The root mean square (RMS) value of the mixture fraction fluctuation, ξ', is around 1% of $\langle\xi\rangle$. The Damköhler number, $\mathrm{Da} = (l_0/\delta_F)/(u'/S_L)$, and Karlovitz number, $\mathrm{Ka} \approx (u'/S_L)^{3/2}/(l_0/\delta_F)^{-1/2}$, are respectively 0.69 and 11.9, where S_L is the burning velocity of a representative unstrained laminar flame and δ_F is the Zeldovich thickness. This turbulent MILD combustion corresponds to Case B in [21] and Case B1 in [24]. The laminar flame, called as MIFE (MILD Flame Element) in [24], has a reactant mixture composition with major species mass fraction values equal to volume averaged values in the inflowing mixture used for the DNS. Thus, the reactant mixture in MIFE includes the recirculated gas mixture excluding minor species. The burning velocity, thermal thickness, $\delta_{th} = (T_p - T_r)/|\nabla T|_{\max}$, and δ_F of MIFE are 1.66 m/s, 1.29 mm and 0.22 mm respectively.

The DNS domain is cubic of size $L_x \times L_y \times L_z = 10 \times 10 \times 10\,\mathrm{mm}^3$ with inflow and non-reflecting outflow boundaries specified using Navier–Stokes characteristic boundary condition [28] in x and periodic conditions in y and z directions. This computational domain is discretised using $N_x \times N_y \times N_z = 384 \times 384 \times 384$ grid points. These grid points ensured that there are about 25 grid points inside the thermal thickness, δ_{th}, and 2 mesh points inside the Kolmogorov length scale. The simulation was run for 1.5 flow-through time, τ_D, before collecting data for statistical analysis. The simulation was then continued for one additional flow-through time and 80 data sets were collected for detailed analyses. Elaborate discussion of this DNS data can be found in Ref. [21,24]. The DNS results are investigated using instantaneous and filtered fields in the following sections. An investigation regarding RANS modelling of this DNS data is reported in [29].

3. LES filtering operation and presumed PDF

For the present analysis, a quantity $f(\mathbf{x})$ obtained from the DNS data is filtered using

$$\overline{f}(\mathbf{x}) = \int f(\mathbf{x}')G(\mathbf{x}-\mathbf{x}';\Delta)\quad d\mathbf{x}', \tag{2}$$

where $\mathbf{x}$ is a spatial vector and G is the Gaussian kernel with filter size Δ given by

$$G(\mathbf{x}-\mathbf{x}';\Delta) = \left(\frac{6}{\pi\Delta^2}\right)^{1/2}\exp\left[\frac{-6(\mathbf{x}-\mathbf{x}')^2}{\Delta^2}\right]. \tag{3}$$

The Favre filtered quantity is obtained using $\widetilde{f} = \overline{\rho f}/\overline{\rho}$ and the variance of Favre fluctuation is $\widetilde{f''^2} = \overline{\rho(f-\widetilde{f})^2}/\overline{\rho}$.

The presumed PDF, $P_\beta(\zeta)$, where ζ is the sample space variable for c, is computed using the β-function with given values of $\widetilde{c}$ and $\widetilde{c''^2}$ as:

$$P_\beta(\zeta) = \frac{\zeta^{r-1}(1-\zeta)^{s-1}}{I_b}, \tag{4}$$

$$I_b = \int_0^1 \zeta^{r-1}(1-\zeta)^{s-1}\quad d\zeta = \frac{\Gamma(r)\Gamma(s)}{\Gamma(r+s)}, \tag{5}$$

$$r = \frac{\widetilde{c}^2(1-\widetilde{c})}{\widetilde{c''^2}} - \widetilde{c}, \quad s = \frac{r(1-\widetilde{c})}{\widetilde{c}}. \tag{6}$$

The values of $\widetilde{c}$ and $\widetilde{c''^2}$ are obtained from the DNS data using Eq. (2) in this study, and these values would be obtained by solving their transport equations in actual LES.

4. Results and discussion

4.1. DNS results

The RPV is defined as $c_T = (T - T_r)/(T_p - T_r)$ for this study and thus the reaction rate is given by $\omega_{c_T} = Q/c_p(T_p - T_r)$, where Q and c_p are the heat release rate and specific heat capacity respectively. A typical spatial variation of this reaction rate normalised using $\rho_r S_L/\delta_{th}$, where ρ_r is the reactant mixture density, in the middle x-y plane is shown in Fig. 1 for $t = 1.5\tau_D$. The superscript "+" here and in the following discussion denotes normalised quantities using laminar flame values appropriately. For example, length and reaction rate are normalised using $1/\delta_{th}$ and $\rho_r S_L/\delta_{th}$. In Fig. 1,

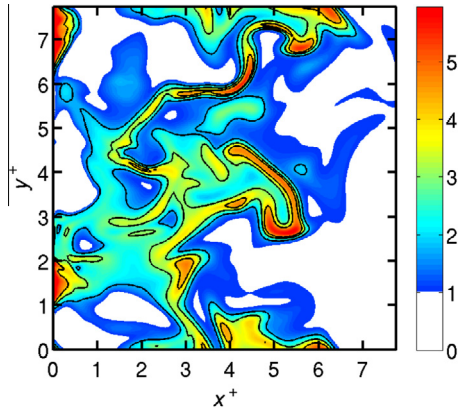

Fig. 1. Typical variation of normalised reaction rate $\omega^+_{c_T}$ in the middle x-y plane at $t = 1.5\tau_D$. Contours of $\widehat{\omega}_{c_T} = 0.3$, 0.5 and 0.7 are shown for clarity, where $\widehat{\omega}_{c_T} = \omega_{c_T}/\omega_{c_T,\max}$ and $\omega_{c_T,\max}$ is the maximum reaction rate in the domain.

regions having $\omega^+_{c_T} > 1$ occupy a substantial part of the computational volume. Although intense reaction zones (see $\widehat{\omega}_{c_T} = \omega_{c_T}/\omega_{c_T,\max} = 0.5$ contour) seem to have thin structures locally, these reaction zones are highly convoluted resulting in their inevitable interactions and such interactions yield distributed reaction zones combustion ([11]). The contour of several $\omega^+_{c_T}$ levels show a patchy appearance of reaction zones spread throughout the domain. Similar behaviour of reaction zones in MILD combustion may be perceived using OH Planar Laser Induced Fluorescence (PLIF) images in [10].

The PDF of c_T, in RANS context, constructed using samples collected in y-z plane at a given x location and from the entire sampling period is shown in Fig. 2 for several $x^+ \equiv x/\delta_{th}$ locations. Although this PDF shows a large probability of finding unburnt gases at $x^+ = 0.30$, its variation is generally broad. Especially, the PDF at $x^+ = 4.1$ has a plateau suggesting a relatively uniform temperature distribution without strong scalar gradients [1–3]. The PDF peak increases and shifts towards larger c_T as seen in Fig. 2 if one moves further downstream through the computational domain. Also, the PDF remains broad with non-zero probability for $0.5 \leqslant c_T \leqslant 1$. The bimodal behaviour for this PDF is not observed implying that the use of classical flamelets to model mean reaction rate in MILD combustion may not be fully acceptable and alternative approaches are to be found. It is worth noting here that this non-flamelet like PDF can also result from frequent and extensive interactions of thin flames, producing an intense reaction rate but a decrease in the local scalar gradient [11]. Thus, the influence of interactions on flamelets must be taken into account.

The sub-grid PDF, $P_\Delta(c_T)$, constructed using samples collected within the filter volume of Δ^3 using the DNS data at $t = 1.5\tau_D$ is shown in Fig. 3. The centre of this volume is used to

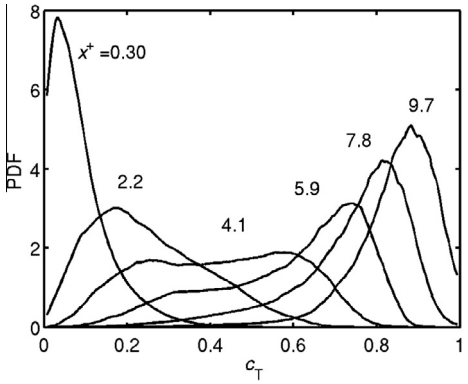

Fig. 2. The PDF of c_T is shown for several streamwise (x) locations. This RANS PDF is constructed using data collected over entire sampling period.

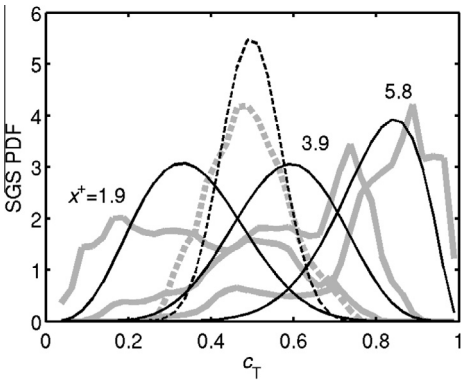

Fig. 3. The sub-grid PDF, $P_\Delta(c_T)$, for three streamwise positions $x^+ = 1.9$, 3.9 and 5.8. Thick grey lines are explicitly filtered DNS values and thin lines are modelled values. Solid line: $\Delta = 3\delta_{th}$, and dashed line: $\Delta = \delta_{th}$ (shown only for $x^+ = 3.9$).

indicate location of this PDF in this figure and three such locations are noted. Two filter sizes, $\Delta = \delta_{th}$ and $3\delta_{th}$, are used. The result for $x^+ = 3.9$ is shown for both of these two filter sizes and it is shown only for $\Delta = 3\delta_{th}$ for the other two locations in Fig. 3. The thick lines represent the DNS results and the thin lines are modelled PDFs, $P_\beta(c_T)$, calculated using the β function in Eqs. (4)–(6) for the values of $\widetilde{c}_T$ and $\widetilde{c''^2_T}$ obtained from the DNS data. The sub-grid PDFs also show neither bimodality nor uniform distribution and the non-smooth variation of P_Δ is because of limited samples from one snap-shot of the DNS data used for the analysis. This specific comparison is shown here so that a "true" behaviour at a given time (in a single snap-shot) can be studied without the influence of time averaging.

The PDF is narrow for $\Delta = \delta_{th}$ and it is broad for the wider, $\Delta = 3\,\delta_{th}$ filter used. These variations are represented reasonably by the modelled PDF, P_β. The sub-grid PDFs obtained using the DNS data collected over the entire sampling period are used to verify the closure model in Eq. (1) for the filtered reaction rate in the discussion below.

4.2. Perfectly Stirred Reactor model

Both the RANS and sub-grid PDFs studied in the previous section suggest that the MILD combustion conditions considered in this study involve distributed reaction zones regime combustion. This regime for MILD combustion is not because of idealised homogeneous reactive mixture but due to interacting flamelets having common features of conventional combustion and some distinctive characteristics of their own, for example the interplay between autoignition and flame propagation [21]. These physical processes

result in small scalar gradients which are not the usual signature of typical flamelet combustion [21]. Based on these observations, a PSR having a residence time representative of local fluid dynamic conditions is explored here. Although a similar model was used in a previous LES study [19], its direct assessment has not been conducted hitherto and thus it is investigated in this study. The initial diluted reactant mixture composition is based on volume averaged mass fraction values for all species present in the initial/inflowing mixture field used for the DNS. Note that the PSR mixture composition is not exactly the same as that of MIFE for which only the minor species are excluded to avoid reactions at the inflow boundary [21]. Since this PSR is modelled as an unsteady homogeneous reactor and ξ' is very small, the only independent variable time, t, is converted to RPV through $c_T(t) = (T(t) - T_r)/(T_p - T_r)$, where $T(t)$ is the temperature of the reactor at time t and T_p is the reactor temperature when the residence time is very large. This zero dimensional unsteady PSR governing equations with initial conditions $T_r = T_m$ and $Y_i = \langle Y_{i,r} \rangle$ (including recirculated gases containing radicals) are integrated in time using COSILAB [30] until $T(t)$ reaches a steady value. Here, the residence time is equal to the mean convection time τ_D from the inflow to outflow boundaries in the DNS. Note that residence times ranging from $\tau_D/4$ to τ_D are also considered but it does not change the $c_T - \omega_{c_T}$ relationship unduly, although maximum value of c_T becomes lower with a decrease in residence time. Also, it is found that the temperature of the PSR with a residence time of τ_D is similar to T_p despite a difference in minor species composition between MIFE and PSR. The same chemical kinetics employed for the DNS is also used for the PSR calculations. The ignition delay time defined based on the instant of maximum temperature rise is about 0.35 ms and this relatively short delay time is due to the presence of radicals and intermediates in the initial mixture.

The variations of Y_i and $\omega^+_{c_T}$ with c_T are shown in Fig. 4. The scattered data is from the DNS result taken at $t = 1.5\tau_D$ from the entire DNS domain and it shows a larger scatter for Y_i and ω_{c_T} near $c_T \sim 0$. The range for this scatter decreases as c_T increases due to the progress of turbulent mixing, molecular diffusion and chemical reactions. The general trend for the variation of DNS quantities with c_T shown in Fig. 4 is represented by the conditional averages, $\langle Y_i|c_T \rangle$ and $\langle \omega^+_{c_T}|c_T \rangle$ shown in this figure. These conditional averages are computed using samples collected over the entire sampling period. The values of $\langle Y_{CH_4}|c_T \rangle$ decreases as the temperature increases. The conditional OH mass fraction is non-zero even for small c_T values, which results from the mixing of OH present in the exhaust gases with reactant. This leads to non-zero $\langle \omega^+_{c_T}|c_T \rangle$ even

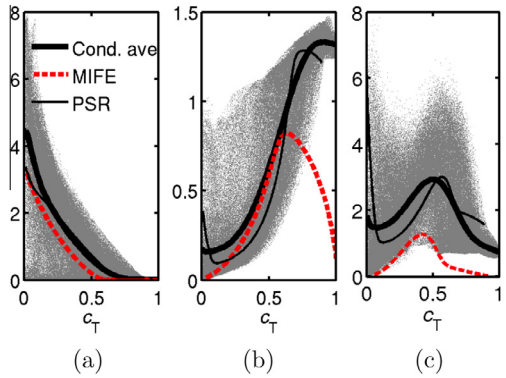

Fig. 4. Variations of (a) Y_{CH_4} ($\times 10^3$), (b) Y_{OH} ($\times 10^3$) and (c) $\omega^+_{c_T}$ with c_T. The scattered data is the DNS result at $t = \tau_D$, thick solid line is the conditional averages, $\langle Y_i|c_T \rangle$ (a and b) and $\langle \omega^+_{c_T}|c_T \rangle$ (c), obtained from the DNS data collected over the entire sampling period, red dashed line is the flamelet (MIFE) solution, and thin solid line is the PSR result. (For interpretation of the references to color in this figure legend, the reader is referred to the web version of this article.)

for $c_T \sim 0$ suggesting that local mixtures start to react as soon as they enter the computational domain. This is because of high T_r and presence of chemically active radicals near the inlet, as one would expect in MILD combustion because of recirculation of exhaust gases. These reaction zones near the inlet are spatially non-uniform, $\langle \omega^+_{c_T}|c_T \rangle$ values in the DNS are smaller than the PSR value for $c_T \simeq 0$. However, there are some samples in the DNS with as large $\omega^+_{c_T}$ as in the PSR near $c_T \simeq 0$.

The results for the two models involving flamelets (MIFE) and PSR are compared with the DNS results in Fig. 4. Although the MIFE solution represents the variations of Y_{CH_4} well the comparisons shown for Y_{OH} and reaction rate are not good as in Fig. 4. Similar comparisons are observed for other major and minor species mass fractions values (not shown). The disagreement seen for the minor species and reaction rate is because of the presence of radicals and intermediates in the inflowing mixture field for the DNS. These species cannot be included for the MIFE, because the flame speed eigenvalue does not exist when the radical and intermediates are present in the reactant mixture at high temperature such as in MILD combustion [31]. Although the inflowing mixture is non-uniform, the zero-dimensional PSR model gives reasonable agreement with the conditional averages of both the major and minor species mass fraction values, and reaction rate (only Y_{CH_4} and Y_{OH} are shown in Fig. 4). The reaction rate for low c_T values is significantly large for the PSR model compared to the DNS values. This significant difference is due to the boundary conditions; radicals are confined to a relatively

small portion creating non-uniform reaction rate field for low c_T value which occurs near the inflow boundary of the DNS domain. However, good comparisons seen in Fig. 4 suggest that the PSR model is a suitable candidate for the MILD conditions investigated in this study.

5. *A priori* assessment

The filtered reaction rate of c_T is modelled using Eq. (1) and the β PDF in Eqs. (4)–(6). This modelled value is denoted as $\overline{\omega}^+_{c_T,\text{model}}$ in the following discussion. This modelled reaction rate field is compared to the filtered reaction rate $\overline{\omega}^+_{c_T}$ obtained by explicitly filtering the DNS results using Eq. (2). The values of $\widetilde{c}$ and $\widetilde{c''^2}$ required for the β PDF model are obtained by filtering the DNS values appropriately. Three values of filter widths, $\Delta = \delta_{th}, 2\delta_{th}$ and $3\delta_{th}$, are used for the assessment discussed in this subsection.

Figure 5 shows a comparison of $\overline{\omega}^+_{c_T}$ and $\overline{\omega}^+_{c_T,\text{model}}$ in the middle x-y plane at $t = 1.5\tau_D$ for $\Delta = \delta_{th}, 2\delta_{th}$ and $3\delta_{th}$. Note that this plane is the same as in Fig. 1, but only a small part, $2 \leqslant y^+ \leqslant 6$, is shown for a better comparison. Small convoluted islands of intense reaction rates observed in Fig. 1 become smoothed due to filtering operation to construct $\overline{\omega}^+_{c_T}$. The smoothing becomes more obvious as the filter size increases, which yields an appearance of distributed reaction zones with $\overline{\omega}^+_{c_T} \geqslant 1$ spreading over a large portion of the domain. The modelled reaction rate $\overline{\omega}^+_{c_T,\text{model}}$ seems to reproduce the filtered reaction rate field reasonably well as shown in Fig. 5. However, the model underestimates the filtered reaction rate near the inflow boundary.

The performance of this reaction rate model in a broader context can be examined by studying the joint PDF (JPDF) of $\overline{\omega}^+_{c_T}$ and $\overline{\omega}^+_{c_T,\text{ model}}$. This JPDF is shown in Fig. 6 for three filter widths. If there is a perfect agreement between the modelled and DNS values of the filtered reaction rate then this JPDF will have a spread around the diagonal lines shown in this figure. As one can observe in Fig. 6, there is an increased tendency

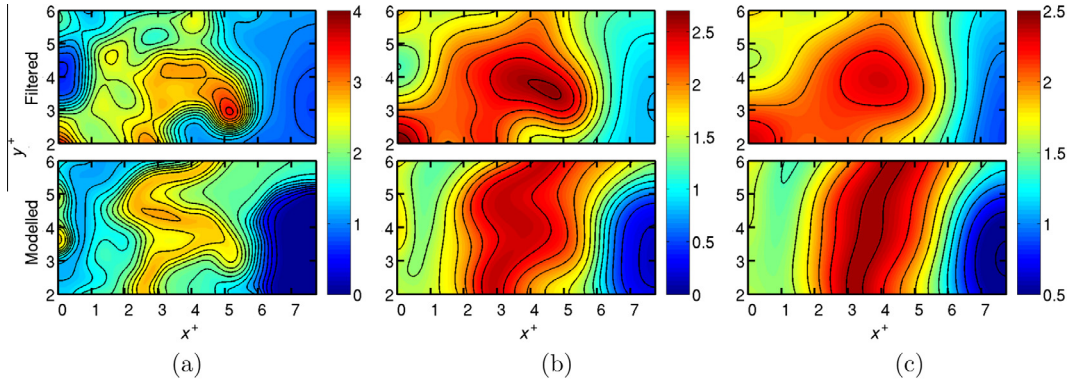

Fig. 5. Comparison of $\overline{\omega}^+_{c_T}$ (top) and $\overline{\omega}^+_{c_T,\text{model}}$ (bottom) in the middle x-y plane at $t = 1.5\,\tau_D$ for (a) $\Delta = \delta_{th}$, (b) $2\delta_{th}$ and (c) $3\delta_{th}$. Note that this plane is the same as in Fig. 1, but only $2 \leqslant y^+ \leqslant 6$ is shown.

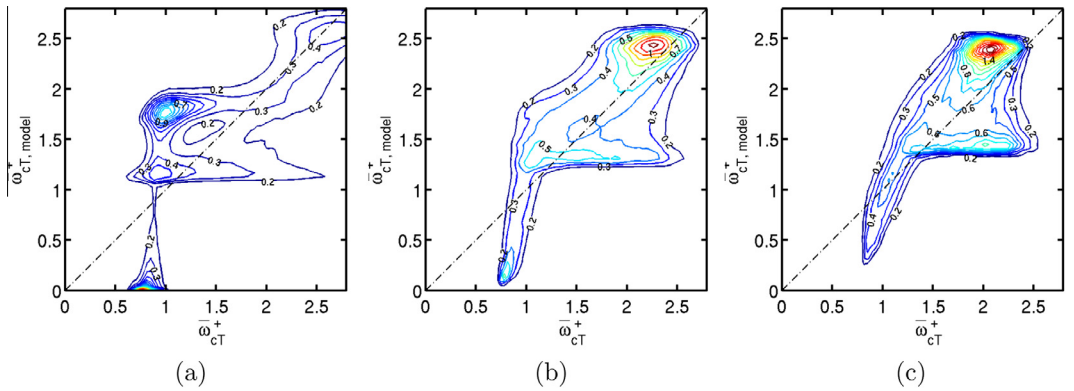

Fig. 6. The JPDF of $\overline{\omega}^+_{c_T}$ and $\overline{\omega}^+_{c_T,\text{ model}}$ computed using the DNS data from the entire sampling period for (a) $\Delta = \delta_{th}$, (b) $2\delta_{th}$ and (c) $3\delta_{th}$.

for this spread for larger filter widths. The reason for this is as follows. The conditions of the current MILD combustion case include both thin and distributed reaction zones as seen in Fig. 1. Most of these thin reaction zones are filtered out for $\Delta = 2\delta_{th}$ and $3\delta_{th}$, while they are likely to remain for $\Delta = \delta_{th}$. Obviously, the PSR model does not cater for thin reaction zones resulting in a poor comparison for $\Delta = \delta_{th}$ as seen in Fig. 6a. These results suggest that the PSR model with a standard presumed PDF approach works reasonably well for MILD combustion modelling. The classical flamelets model may have to be extended to include effects of flame interactions before it could be used for turbulent MILD combustion.

6. Summary

DNS data of turbulent MILD combustion of methane are analysed to construct a simple model for filtered reaction rate required for Large Eddy Simulations. This analysis showed that reaction zones in MILD combustion are spread over large portion of the computational domain and are partly thin structures having some common features of conventional premixed combustion. These thin structures interact frequently giving an appearance of distributed regime combustion. These views expressed in an earlier study [21] are supported further by the marginal PDF of normalised temperature, c_T. Both sub-grid and RANS PDFs are analysed and β function PDF modelled using Favre filtered c_T and its sub-grid variance obtained from the DNS data is found to be a reasonable model.

The conditionally averaged species mass fractions and reaction rate for c_T constructed from the DNS data are compared to those obtained from flamelet and PSR models. A flamelet, called as MIFE, having the reactant mixture composition corresponding to the DNS mixture is used. The residence time for the unsteady PSR model has a broad range to cover all possible reacting state that could exist in turbulent MILD combustion for thermochemical and turbulence conditions considered here. Although the flamelet model compares well with DNS data for major species mass fractions, the conditional averages of minor species mass fractions and reaction rates do not compare well. This could be due to the presence of flame interactions which are not included in the flamelets model. The avenues to include effects of interaction in flamelets based approach are unclear and it is an open question at this time. However, it would also be interesting to compare turbulent MILD reaction zones with canonical reaction zones other than MIFE and PSR, such as Homogeneous Charge Diffusion Ignition (HCDI) [32]. The PSR results compare very well for major and minor species mass fractions, and reaction rate. Thus, this model along with the presumed β sub-grid PDF is used to find a simple closure for filtered reaction rate. This modelled reaction rate field and that obtained by filtering the DNS result agree reasonably well for filter size of $\Delta \geqslant 3\delta_{th}$.

Acknowledgements

Y. M. acknowledges the financial support of Nippon Keidanren. EPSRC support is acknowledged. This work made use of the facilities of HECToR, the UK's national high-performance computing service, which is provided by UoE HPCx Ltd at the University of Edinburgh, Cray Inc and NAG Ltd, and funded by the Office of Science and Technology through EPSRC's High End Computing Programme.

References

[1] M. de Joannon, A. Saponaro, A. Cavaliere, *Proc. Combust. Inst.* 28 (2000) 1639–1646.
[2] I.B. Özdemir, N. Peters, *Exp. Fluids* 30 (2001) 683–695.
[3] N. Krishnamurthy, P.J. Paul, W. Blasiak, *Proc. Combust. Inst.* 32 (2009) 3139–3146.
[4] J.A. Wünning, J.G. Wünning, *Prog. Energy Combust. Sci.* 23 (1997) 81–94.
[5] A. Cavaliere, M. de Joannon, *Prog. Energy Combust. Sci.* 30 (2004) 329–366.
[6] M. de Joannon, P. Sabia, A. Tregrossi, A. Cavaliere, *Combust. Sci. Technol.* 176 (2004) 769–783.
[7] M. de Joannon, A. Cavaliere, T. Faravelli, E. Ranzi, P. Sabia, A. Tregrossi, *Proc. Combust. Inst.* 30 (2005) 2605–2612.
[8] P. Sabia, M. de Joannon, S. Fierro, A. Tregrossi, A. Cavaliere, *Exp. Thermal Fluid Sci.* 31 (2007) 469–475.
[9] T. Plessing, N. Peters, J.G. Wünning, *Proc. Combust. Inst.* (1998) 3197–3204.
[10] B.B. Dally, E. Riesmeier, N. Peters, *Combust. Flame* 137 (2004) 418–431.
[11] Y. Minamoto, T.D. Dunstan, N. Swaminathan, R.S. Cant, *Proc. Combust. Inst.* 34 (2013) 3231–3238.
[12] R. Weber, S. Orsino, N. Lallemant, A. Verlaan, *Proc. Combust. Inst.* 28 (2000) 1315–1321.
[13] S. Orsino, R. Webber, U. Bollettini, *Combust. Sci. Technol.* 170 (2001) 1–34.
[14] F.C. Christo, B.B. Dally, *Combust. Flame* 142 (2005) 117–129.
[15] C. Galletti, A. Parente, L. Tognotti, *Combust. Flame* 151 (2007) 649–664.
[16] P. Li, J. Mi, *Flow Turbulence Combust.* 33 (2011). http://dx.doi.org/10.1007/s10494-011-9348-x.
[17] J. Aminian, C. Galletti, S. Shahhosseini, L. Tognotti, *Appl. Thermal Eng.* 31 (2011) 3287–3300.
[18] Y. Afarin, S. Tabejamaat, *Combust. Sci. Technol.* 17 (2013) 383–410.
[19] C. Duwig, D. Stankovic, L. Fuchs, G. Li, E. Gutmark, *Combust. Sci. Technol.* 180 (2008) 279–295.

[20] M. Ihme, Y.C. See, *Proc. Combust. Inst.* 33 (2012) 1309–1317.
[21] Y. Minamoto, N. Swaminathan, *Combust. Flame* 161 (2014) 1063–1075.
[22] R.S. Cant, in: Technical Report CUED/A–THERMO/TR67, Cambridge University Engineering Department, 2012.
[23] M.D. Smooke, V. Giovangigli, in: M.D. Smooke (Ed.), *Reduced kinetic mechanisms and asymptotic approximations for methane–air flames*, vol. 384, Springer Verlag, New York, 1991, pp. 1–28.
[24] Y. Minamoto, N. Swaminathan, R.S. Cant, T. Leung, *Combust. Sci. Technol.* (2014). http://dx.doi.org/10.1080/00102202.2014.902814.
[25] E. Oldenhof, M.J. Tummers, E.H. van Veen, D.-J.E.M. Roekaerts, *Combust. Flame* 158 (2011) 1553–1563.
[26] C. Duwig, B. Li, M. Aldén, *Combust. Flame* 159 (2012) 306–316.
[27] P.R. Medwell, Laser diagnostics in MILD combustion, Ph.D. thesis, The University of Adelaide, Adelaide, Australia, 2007.
[28] T. Poinsot, S. Lele, *J. Comput. Phys.* 101 (1992) 104–129.
[29] Y. Minamoto, N. Swaminathan, *Int. J. Adv. Eng. Sci. Appl. Math.* (2014). http://dx.doi.org/10.1007/s12572-014-0106-x.
[30] COSILAB, The Combustion Simulation Laboratory Version 2.0.8, 2007. Rotexo-Softpredict-Cosilab GmbH & Co. KG, Germany.
[31] J. Sidey, E. Mastorakos, R.L. Gordon, *Combust. Sci. Technol.* 186 (2014) 453–465.
[32] M. de Joannon, A. Matarazzo, P. Sabia, A. Cavaliere, *Proc. Combust. Inst.* 31 (2007) 3409–3416.